Unusual Evolutions of Dissipative-Soliton-Resonance Pulses in an All-Normal Dispersion Fiber Laser

Yufei Wang,[1] *Student Member, IEEE,* Lei Li,[1] Junqing Zhao,[1] Shuai Wang,[1] Chaojie Shu,[1] Lei Su,[2] Dingyuan Tang,[1] Deyuan Shen,[1] and Luming Zhao,[1,2] *Senior Member, IEEE*

[1]Jiangsu Key Laboratory of Advanced Laser Materials and Devices, Jiangsu Collaborative Innovation Center of Advanced Laser Technology and Emerging Industry, School of Physics and Electronic Engineering, Jiangsu Normal University, Xuzhou, Jiangsu 221116, China

[2]School of Engineering and Materials Science, Queen Mary University of London, London, UK

Abstract: We experimentally report novel evolutions of dissipative-soliton-resonance (DSR) pulses with respect to the pump power in an all-normal-dispersion fiber laser based on a nonlinear optical loop mirror (NOLM). By solely increasing the pump power, pulse breaking of DSR pulses was observed apart from the typical pulse broadening at a fixed pulse peak power. Instead of arbitrarily broadening with the increase in the pump power or directly losing the mode-locking state, the process of pulse breaking was accompanied by the multi-pulse state and harmonic mode-locking (HML) pulses evolving from the original DSR pulse. In addition, to the best of our knowledge, a narrowing of the DSR pulse with the increase in the pump power was observed for the very first time. Further results show that these unusual evolutions of DSR pulses could be attributed to the changes in several laser parameters resulting from the increasing pump power under specific operating conditions.

Index Terms: Fiber Lasers, Optical Solitons, Optical pulses.

1. Introduction

Passively mode-locked fiber lasers have been widely considered for ultrashort pulse generation owing to their compact, versatile, and alignment-free characteristics. Studies on obtaining high-energy pulse output from passively mode-locked lasers are ongoing both in academia and in the industry. However, the wave breaking phenomenon restricts increasing the pulse energy because of the considerable accumulated nonlinear effect, which leads to pulse splitting.

To circumvent the wave breaking phenomenon, dissipative soliton resonance, which is a square-like pulse formation mechanism theoretically proposed by Chang *et al*. (2008) [1], has attracted significant attention in the past decade. Within the DSR regime, the peak of the pulse remains constant while the pulse width broadens linearly with the increase in the pump power. According to the DSR phenomenon, the pulse energy can be indefinitely increased as long as the pulse width arbitrarily broadens without pulse splitting. Both theoretical analysis and various experiments have proven that under an appropriate set of cavity parameters, the generation of DSR is independent of the cavity dispersion and mode-locking technique [2-15]. Li et al. proved that the DSR pulse is compressible which could lead to higher peak power [11]. The level of DSR pulse energy directly from a fiber laser has exceeded tens of micro joules by using a double-cladding fiber amplifier [15]. Using the master oscillator power amplifier (MOPA) to amplify the DSR pulse, the pulse energy can exceed 90 μJ when average output power reaches 100 W [10]. DSR is a specific parameter space among the short-pulse fiber lasers to achieve large pulse energy. Investigating the characteristics and dynamics of DSR pulses will facilitate their potential applications. In practice, increasing the pump power not only increases the effective gain, but also leads to changes in other parameters such as the central wavelength, cavity birefringence, and continuous wave (CW). Therefore, the DSR pulse can evolve differently with respect to the pump power, contrary to theoretical predictions.

If the DSR pulse is out of its original parameter space during the broadening process, its wave-breaking-free properties will be destroyed. Multi-pulse state caused by pulse splitting may occur [16]. Multiple pulses have been observed and discussed in different passively mode-locked fiber lasers [16-20]. Novel techniques such as dissipative faraday instability [21] and Mamyshev oscillator [22] can produce stable multiple pulses with high repetition rate in fiber lasers. In the DSR regime, multi-pulse state of DSR harmonic mode-locking have been investigated theoretically [23] and experimentally [24–28]. Komarov et al. concluded that the number of DSR pulses in the steady state is related to the initial conditions, regardless of the increasing pump power [23]. Recently, Chowdhury et al. demonstrated the multiple DSR pulses in a single round trip in the all-normal dispersion regime [29].

In this paper, we report on the pulse dynamics of single DSR pulse evolution with respect to the pump power in an all-normal dispersion fiber laser with a nonlinear fiber loop mirror. First, the DSR characteristic, i.e., the broadening pulse duration, is studied at a constant pulse peak power. With further increase in the pump power, we check whether the DSR performance can be maintained while keeping the other laser configurations unchanged. Solely increasing the pump power may result to the change of multiple parameters, different DSR evolutions including dual DSR pulse generation and HML states of DSR

pulses can be expected. Considering the possibility of decrease in the effective gain because of the combined effects resulting from the increase in pump power, DSR pulse narrowing is likely to be realized.

2. Experimental setup

Fig. 1 shows the schematic of the all-normal dispersion fiber laser used in our experiment. An NOLM, which acts as a fast saturable absorber, is coupled into a unidirectional ring (UR) cavity through a 30/70 fiber coupler (OC). The NOLM comprises a polarization controller (PC1) and a 200-m-long single-mode fiber (SMF, Nufern, 1060-XP) to enhance the nonlinear effects. In the UR, the gain is provided using a 30-cm-long single-cladding, ytterbium-doped fiber (YDF, CorActive Yb501) with a core absorption 139 dB/m at 915 nm. The net cavity dispersion is about 5.482 ps^2. The YDF is pumped through a wavelength division multiplexer (WDM) using a 976 nm pigtailed laser diode, providing a maximum pump power of 600 mW. A polarization-independent isolator (PI-ISO) is inserted into the UR to ensure unidirectional operation and prevent backward reflections. Another polarization controller (PC2) is used to adjust the intra-cavity polarization state. A fiber coupler with 20% port acting as an output is placed after PC2. The fiber pigtail of all the optical components in this laser is HI1060. The total length of the laser is 229 m, corresponding to a fundamental repetition rate of ~900 kHz. A 63 GHz high-speed oscilloscope (Agilent, DSA-X 96204Q) along with a 45-GHz photodetector (New Focus, 1014) is employed to visualize the output pulse train. The spectrum is analyzed using an optical spectrum analyzer (OSA, Yokogawa AQ6317C). The output power is monitored using an optical power meter (Agilent, 81681A), and the radio-frequency (RF) spectra are measured using an RF-spectrum analyzer (Agilent, N9320B).

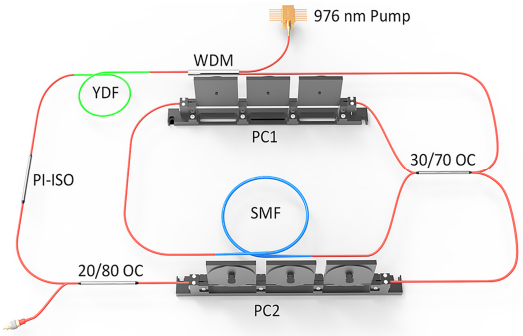

Fig. 1. Schematic of the all-normal dispersion fiber laser. WDM: wavelength division multiplexer; YDF: ytterbium-doped fiber; PI-ISO: polarization-independent isolator; PC1: polarization controller; OC: fiber coupler; SMF: 200-m-long single-mode fiber.

3. Experimental results and discussion

In our experiment, mode-locked square pulses operating in the DSR regime can be easily obtained at a pump threshold of approximately 40 mW by appropriately adjusting the orientation of the PCs. The mode-locked pulse can be sustained because of the pump hysteresis effect [18,30,31] by decreasing the pump power to 24.5 mW. Fig. 2(a) shows the oscilloscope trace of the mode-locked pulse at a pump power of 24.5 mW, wherein the measured pulse duration is approximately 896 ps. The inset in Fig. 2(a) shows that the pulse train has a uniform interval of 1.11 μs, corresponding to the cavity roundtrip time. The single-pulse temporal profile exhibits an asymmetrical structure, as the pulse front has a higher intensity than the pulse trailing edge. Fig. 2(b) shows the bell-shaped optical spectrum of the mode-locked pulse. This result is consistent with those of previous reports [25,32-35]. The central part of the spectrum shares more gain than the edges. Therefore, the newly generated energy is accumulated at the center. The laser emission is centered at 1034.84 nm with a 0.079 nm 3-dB spectral bandwidth. The calculated time bandwidth product (TBP) is 19.8, implying that the pulse is heavily chirped. According to the RF spectrum, shown in Fig. 2(c), the signal-to-noise ratio exceeds 60 dB at 900 kHz. The inset in Fig. 2(c) shows a broader span of 100 MHz. This confirms that a stable mode-locking operation is achieved.

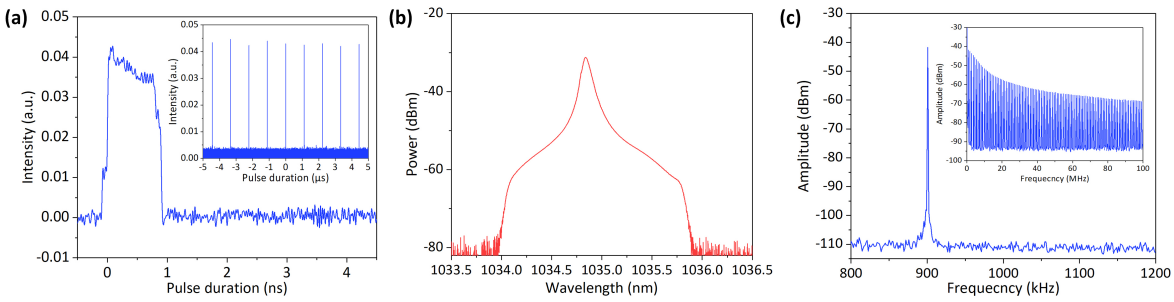

Fig. 2. Typical square-pulse emission under mode-locked threshold. (a) Oscilloscope trace of a single pulse. Inset: the pulse train. (b) Corresponding optical spectrum. (c) RF spectrum with a span of 400 kHz and a resolution bandwidth of 10 Hz. Inset: 100 MHz span, 1 kHz resolution bandwidth.

With fixed PC paddles, the square pulse broadens gradually with the increase in the pump power from 24.5 to 37.7 mW, as shown in Fig. 3(a). The increase in the pulse duration starts at the pulse trailing edge, making the top of the pulse evolve into an extended plateau. The pulse front does not change and still exhibits higher intensity. Fig. 3(b) shows the evolution of the optical spectrum. The central wavelength is found to shift from 1034.84 to 1036.47 nm and the 3-dB spectral bandwidth from 0.079 to 0.047 nm, without using any intra-cavity bandpass filters. A slight increase in the spectral intensity is observed. Fig. 3(d) shows the variations in the average output power, pulse width, pulse energy, and peak power with respect to the pump power. The pulse duration, measured using the fast oscilloscope, increases monotonically from 896 ps to 2.187 ns with the increase in the pump power. Consequently, the average output power and pulse energy increase linearly with respect to the pump power, while the peak pulse power remains largely constant during the broadening process. There is no fine structure in the square profile packet nor any unstable states during this process, observed using the high-speed oscilloscope. As shown in fig.3 (c), we could only achieve an autocorrelation trace at a constant level because of the narrow scanning range of the autocorrelator (FEMTOCHROME, FR 103-HS) compared to the pulse duration at the nanosecond scale. However, no coherent peak with pedestals is observed, thus ruling out the possibility of a noise-like pulse [36]. The above results verify that the pulse operates in the DSR regime.

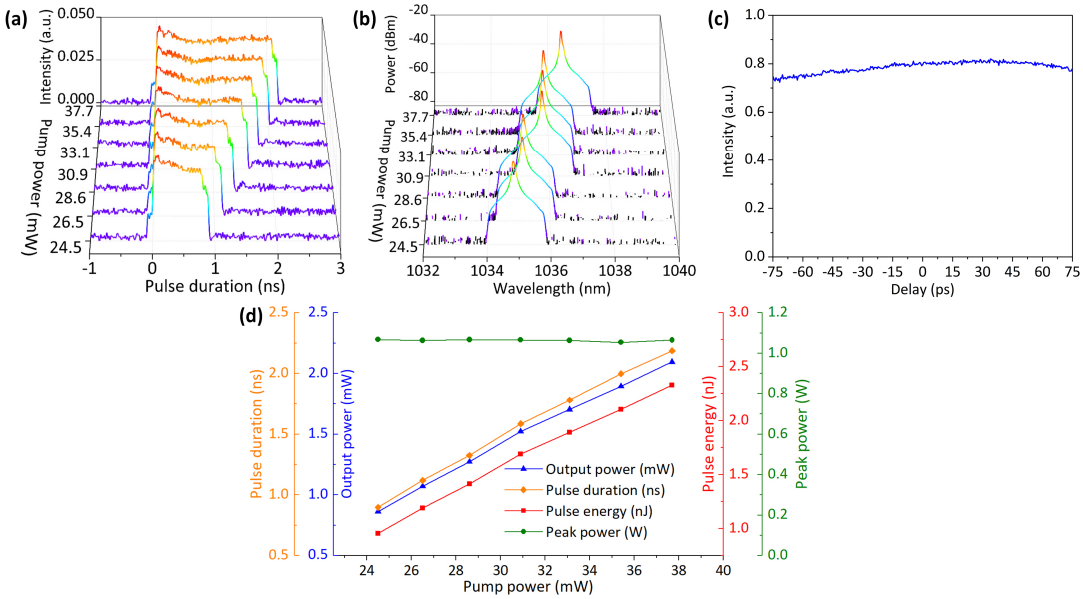

Fig. 3. Square pulse operation in the DSR regime (a) Dynamics of pulse broadening in the time domain. (b) Corresponding optical spectrum with the increase in the pump power. (c) Autocorrelation trace of DSR pulse. (d) Variations in the pulse width, output pump power, pulse energy, and peak power with respect to the pump power.

According to the DSR theory, the linear broadening of the DSR pulse with the increase in the pump power can be maintained. The evolutions of the temporal and spectral profiles of the pulse are further investigated by continuously increasing the pump power from 39.8 to 76.3 mW. Surprisingly, although the pulse keeps broadening with the increase in the pump power, its DSR characteristics can no longer be maintained. In the time domain, as shown in Fig. 4(a), the pulse duration does not increase linearly. The intensity of the flat plateau slightly increases with respect to the pump power, while the pulse front is gradually weakened, thereby changing the asymmetrical structure of the original pulse. The pulse width increases from 2.438 to 3.533 ns. Moreover, notable changes are observed in the optical spectrum in this range of pump power, as shown in Fig. 4(b). At a pump power of 39.8 mW, a secondary signal centered at ~1085 nm is observed in the optical spectrum, apart from the main signal centered at 1036.49 nm. This secondary signal is due to the stimulated Raman scattering (SRS) effect [37-39]. The long-cavity configuration can be attributed to the low threshold required for the onset of SRS [40]. The increase in the pump power not only induces the rise of the SRS components, but also causes blue-shift of both the signal components. A previous report on long-cavity configuration in an all-normal dispersion fiber laser [37] suggests that the advent of SRS can affect the energy scalability, as it takes a part of the pump energy. Moreover, the aggravated SRS can destabilize the pulse in the form of sporadic bursts of intense fluctuations. When the pump power reaches 67.1 mW, a new peak is observed at approximately 1039 nm, which takes a part of the energy of the main signal. The changes in the optical spectrum with the increase in the pump power could explain the evolution of the temporal pulse profile. The output power–pulse width curve plotted as a function of the pump power exhibits nonlinearity, as shown in Fig. 4(c). The variation in the peak power clearly indicates the loss of DSR characteristic. Both the oscilloscope trace and optical spectrum show that the pulse becomes unstable when the pump power is increased to 76.3 mW. The broadening process is terminated, and the average output power changes dramatically at this pump level.

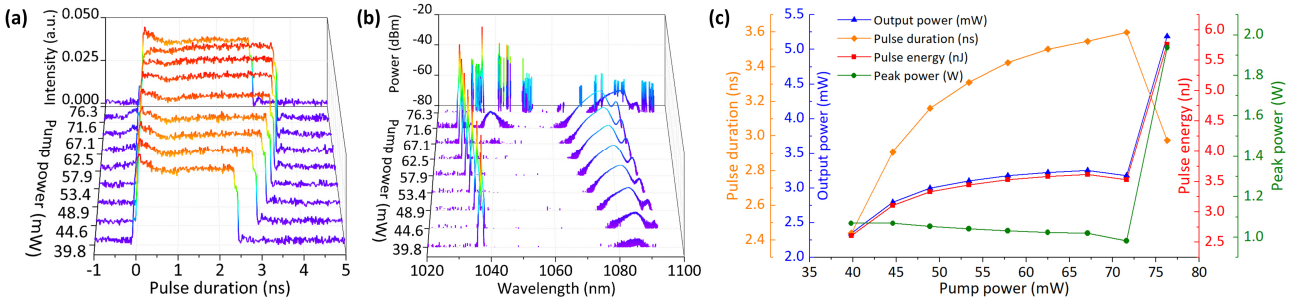

Fig. 4. Pulse broadening out of the DSR regime. (a) Oscilloscope trace of pulse evolution. (b) Corresponding optical spectrum. (c) Variations in the pulse width, output pump power, pulse energy, and peak power with respect to the pump power.

The unstable oscilloscope trace automatically transforms into a steady dual-pulse state when the pump power is slightly increased to 78.5 mW, as shown in Fig. 5(a). The duration of the dual-pulse as a wave-packet is approximately 5 ns. The narrower and wider sub-pulse durations are approximately 0.55 and 3.55 ns, respectively. The sub-pulse separation is approximately 0.9 ns. The inset in Fig. 5(a) shows that the pulse pair has an interval of 1.11 μs, which is consistent with that shown in Fig. 2(a). Fig. 5(b) shows the corresponding RF spectrum. The repetition rate of the pulse pair is still 900 kHz. Figs. 5(c) and (d) show the evolutions of the dual-pulse with the increase in the pump power from 78.5 to 90.1 mW. In the time domain, the structure of the dual-pulse does not change significantly, except when the pump power is increased to 85.4 mW, at which point the pulse duration of the narrower sub-pulse increases to approximately 0.9 ns. In the spectral domain, the spectral component at approximately 1039 nm gradually emerges from the CW substrate with the increase in the pump power. However, the blue shift and ridge of the spectral component are discontinuous, and a jump occurs when the power reaches 85.4 mW. No modulation is observed on the spectrum, implying that there is no interaction between the two sub-pulses.

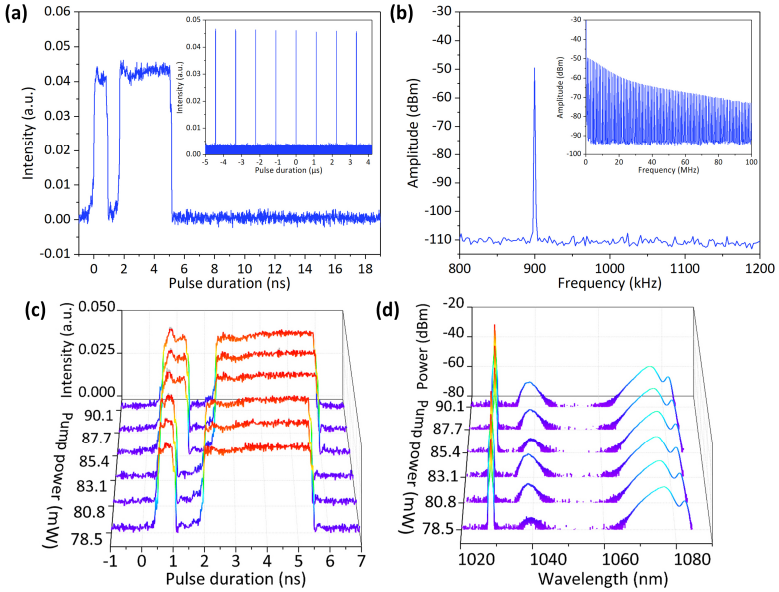

Fig. 5. Square pulse evolves into a dual-pulse state. (a) Oscilloscope trace of a dual-pulse. The inset shows the pulse train at a pump power of 78.5 mW. (b) RF spectrum with a span of 400 kHz and a resolution bandwidth of 10 Hz. Inset: 100 MHz span; 1 kHz resolution bandwidth. (c) Oscilloscope trace of pulse evolution. (d) Corresponding optical spectrum.

Thus far, we found that the initial pulse evolves into a new type of pulse with the continuous increase in the pump power. When the pump power is increased to 92.3 mW, the dual-pulse state evolves into a second-order HML single square pulse, as shown in Fig. 6(a).

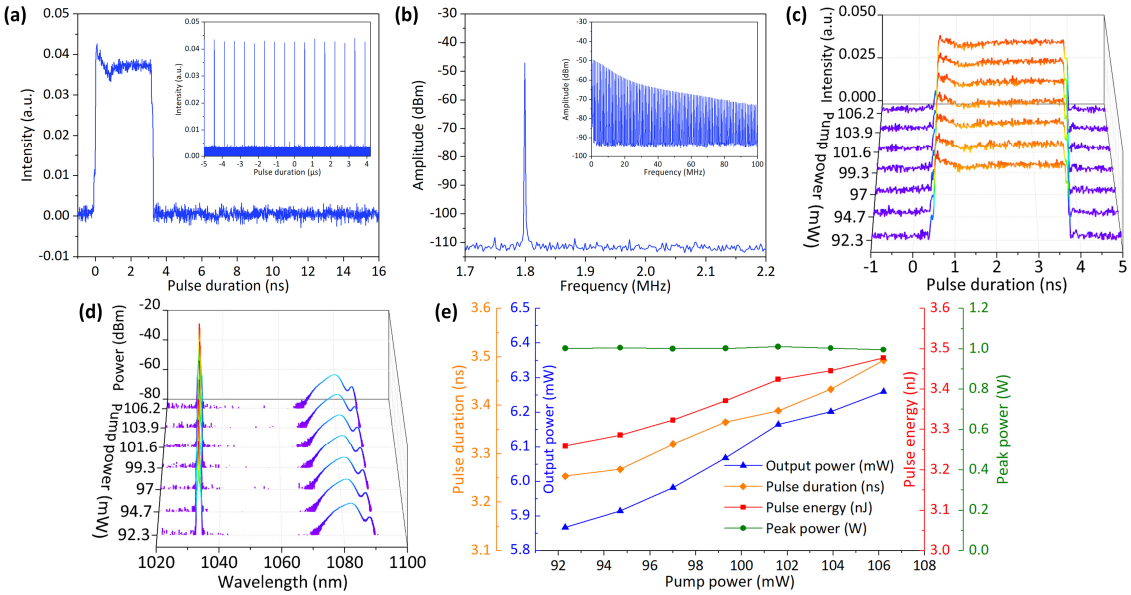

Fig. 6. Second-order harmonic mode-locked square pulse is obtained when the pump power exceeds 92.3 mW: (a) Oscilloscope trace of a harmonic mode-locking pulse. The inset shows the pulse train. (b) RF spectrum with a span of 400 kHz and a resolution bandwidth of 10 Hz. Inset: 100 MHz span; 1 kHz resolution bandwidth. (c) Oscilloscope trace of pulse evolution. (d) Corresponding optical spectrum. (e) Variations in the pulse width, output pump power, pulse energy, and peak power with respect to the pump power.

As shown in the inset of Fig. 6(a), the interval of the uniform pulse train is 555.6 ns, which is half the original DSR pulse interval. As shown in Fig. 6(b), the measured RF spectrum exhibits a signal-to-noise ratio of approximately 60 dB at 1.8 MHz. As shown in Fig. 6(c), with the increase in the pump power from 92.3 to 106.2 mW, the square pulse slightly broadens without any wave-breaking during the process. Compared to the spectrum in the dual-pulse regime, the changes here are evident with the increase in the pump power, as shown in Fig. 6(d). The center wavelength of the pulse changes from 1027.3 to 1033.3 nm during the transition of the pulse from the dual-pulse state to the HML state, respectively. The CW ridge at approximately 1039 nm disappears, whereas the increase in the SRS at approximately 1080 nm still exists. Fig. 6(e) shows that the measured pulse duration increases quasi-linearly with respect to the pump power and that the peak power remains largely constant. However, when the pump power exceeds 106.2 mW, the HML pulse is once again unstable. An unrestricted pump power boost will eventually result in the loss of mode-locked state.

To ensure that the DSR pulse evolution with the increase in the pump power was not accidentally obtained, we reduced the pump power starting from 106.2 mW. As expected, the above phenomenon is still observed in the same order. The pump power is increased and decreased multiple times, and the evolution of the DSR pulse discussed above is consistent with the results obtained here. Fig. 7 shows the entire continuous evolution process.

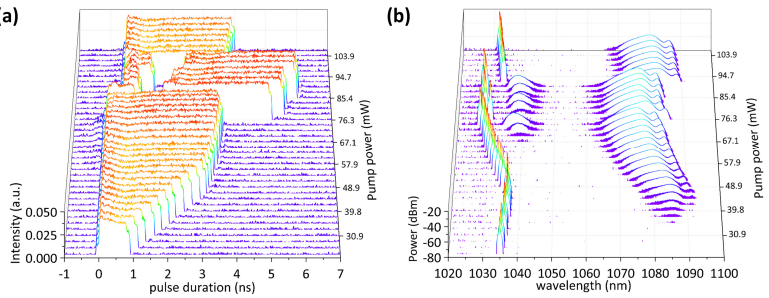

Fig. 7. Tuning the pump power from 24.5 to 106.2 mW (a) Dynamics of pulse evolution in the time domain. (b) Corresponding optical spectrum.

To further investigate the influence of pump power on the DSR pulses, we changed the rotation of the PCs to study the pulse evolution path under different intra-cavity birefringence conditions. Adjusting the PCs varies the balance between gain and loss in the cavity. Specifically, the PC in the NOLM can modulate the linear phase shift between the counter-propagating light [41]. After obtaining the initial DSR pulse, the setting of two PCs are fixed. Only pump power is changed in the evolution. Under a specific PC configuration in our laser, the pulse duration of the DSR pulse does not monotonically increase with the increase in the pump power. Fig. 8(a) shows a special evolution of the temporal profile of the DSR pulse with the increase in the pump power. The figure clearly shows that the linear broadening of the DSR pulse cannot be maintained with the increase in the pump power and that the pulse duration exhibits a saturation trend when the pulse is broadened to a certain extent. The peak of the pulse remains constant during the entire broadening process. From 35.64 to 244.5 mW, the pulse duration changes from 355 ps to 4.214 ns. When the power exceeds 244.5 mW, the pulse no longer continues to broaden but begins

to shrink. With further increase in the pump power, the pulse contraction is faster than the broadening process. Fig. 8(b) shows the change in the spectrum. The entire process is accompanied by a significant wavelength-shift. Unlike the pulse evolution previously discussed, no new frequency components appear on the spectrum. The background noise is enhanced with the increase of the pump power and part of energy would be transferred to the CW, which further affects the gain of the DSR pulse. As a result, the decrease in DSR pulse energy could lead to the pulse shrinkage. Fig. 8(c) shows the variations in the pulse duration, average power, peak power, and pulse energy with respect to the pump power. The pulse broadening process gradually saturates, and the pulse width shrinks rapidly with the continuous increase in the pump power. The peak power fluctuations at the beginning and end of the process are due to the asymmetric structure of the pulse.

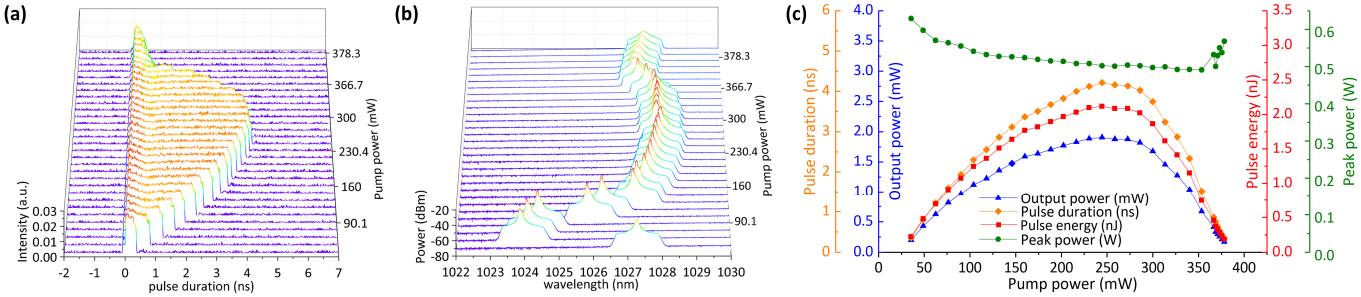

Fig. 8. Tuning the pump power from 35.64 to 244.5 mW (a) Dynamics of pulse broadening and shrinking in the DSR regime. (b) Corresponding optical spectrum. (c) Variations in the pulse width, output pump power, pulse energy, and peak power with respect to the pump power.

4. Conclusion

We experimentally demonstrated a novel evolution of the DSR pulse with the increase in the pump power in an Yb-doped NOLM-based all-normal dispersion fiber laser. In our paper, it is found that under appropriate operating conditions, the original DSR pulse can evolve into a new DSR pulse with a different center wavelength or to a multi-pulse state or an HML state. The birefringence change in the cavity may even cause shrinkage of the DSR pulse with the increase in the pump power. The background noise in the cavity accumulates in the broadening process of DSR pulse. Further increasing the pump power, gain competition leads to the decrease in the gain of DSR pulse. Our findings show that the broadening process of DSR pulse could be unsustainable. In order to overcome these limitations and achieve continuous DSR pulse broadening, further optimizing and manipulating multiple laser parameters would be our future research directions. This study enriches our understanding of the dynamics of DSR phenomenon.

Acknowledgements

Key Research Program of Natural Science of Jiangsu Higher Education Institutions (17KJA416004); National Natural Science Foundation of China (11674133, 11711530208, 61575089, 61705094); Royal Society (IE161214); European Union's Horizon 2020 research and innovation programme under the Marie Skłodowska-Curie grant agreement (790666); Protocol of the 37th Session of China-Poland Scientific and Technological Cooperation Committee (37-17); Priority Academic Program Development of Jiangsu Higher Education Institutions (PAPD); Jiangsu Overseas Visiting Scholar Program for University Prominent Young & Middle-aged Techers and Presidents; Postgraduate Research & Practice Innovation Program of Jiangsu Province (KYCX17_1655).

References

[1] W. Chang, A. Ankiewicz, J. M. Soto-Crespo, and N. Akhmediev, "Dissipative soliton resonances," Phys. Rev. A, vol. 78, no. 2, p. 023830, Aug. 2008.
[2] P. Grelu, W. K. Chang, A. Ankiewicz, J. M. Soto-Crespo, and N. Akhmediev, "Dissipative soliton resonance as a guideline for high-energy pulse laser oscillators," J. Opt. Soc. Am. B, vol. 27, no. 11, pp. 2336–2341, Nov. 2010.
[3] W. Chang, J. M. Soto-Crespo, A. Ankiewicz, and N. Akhmediev, "Dissipative soliton resonances in the anomalous dispersion regime," Phys. Rev. A, vol. 79, no. 3, p. 033840, Aug. 2009.
[4] E. Ding, P. Grelu, and J. N. Kutz, "Dissipative soliton resonance in a passively mode-locked fiber laser," Opt. Lett., vol. 36, no. 7, pp. 1146-1148, Apr. 2011.
[5] L. Duan, X. Liu, D. Mao, L. Wang, and G. Wang, "Experimental observation of dissipative soliton resonance in an anomalous-dispersion fiber laser," Opt. Express, vol. 20, no. 1, pp. 265-270, Jan. 2012.
[6] L. Mei, G. Chen, L. Xu, X. Zhang, C. Gu, B. Sun, and A. Wang, "Width and amplitude tunable square-wave pulse in dual-pump passively mode-locked fiber laser," Opt. Lett., vol. 39, no. 11, pp. 3235–3237, Jun. 2014.
[7] K. Krzempek, "Dissipative soliton resonances in all-fiber Er-Yb double clad figure-8 laser," Opt. Express, vol. 23, no. 24, pp. 30651-30656, Nov. 2015.
[8] H. Yu, X. Wang, P. Zhou, X. Xu, and J. Chen, "High-energy square pulses in a mode-locked Yb-doped fiber laser operating in DSR region," IEEE Photon. Technol. Lett., vol. 27, no. 7, pp. 737–740, Apr. 2015.
[9] G. Semaan, F. B . Braham, J. Fourmont, M. Salhi, F. Bahloul, and F. Sanchez, "10 μJ dissipative soliton resonance square pulse in a dual amplifier figure-of-eight double-clad Er:Yb mode-locked fiber laser," Opt. Lett., vol. 41, no. 20, pp. 4767-4770, Oct. 2016.
[10] J. Zhao, D. Ouyang, Z. Zheng, M. Liu, X. Ren, C. Li, S. Ruan, and W. Xie," 100 W dissipative soliton resonances from a thulium-doped double-clad all-fiber-format MOPA system," Opt. Express, vol. 24, no. 11, pp. 12072-12081, May. 2016.
[11] D. Li, L. Li, J. Zhou, L. Zhao, D. Tang, and D. Shen, "Characterization and compression of dissipative-soliton-resonance pulses in fiber lasers," Sci.

Rep., vol. 6, p.23631, July. 2016.
[12] K. Krzempek, J. Sotor, and K. Abramski, “Compact all-fiber figure-9 dissipative soliton resonance mode-locked double-clad Er:Yb laser,” Opt. Lett., vol. 41, no. 21, pp. 4995-4998, Nov. 2016.
[13] T. Du, Z. Luo, R. Yang, Y. Huang, Q. Ruan, Z. Cai, and H. Xu, “1.2-W average-power, 700-W peak-power, 100-ps dissipative soliton resonance in a compact Er:Yb co-doped double-clad fiber laser,” Opt. Lett., vol. 42, no. 3, pp. 462-465, Feb. 2017.
[14] L. Zhao, D. Li, L. Li, X. Wang, Y. Geng, D. Shen, and L. Su, “Route to Larger Pulse Energy in Ultrafast Fiber Lasers,” IEEE J. Sel. Top. Quantum Electron., vol. 24, no. 3, p.8800409, 2017.
[15] G. Semaan, F. Ben Braham, J. Fourmont, M. Salhi, F. Bahloul, and F. Sanchez, “10 μJ dissipative soliton resonance square pulse in a dual amplifier figure-of-eight double-clad Er:Yb mode-locked fiber laser,” Opt. Lett., vol. 41, no. 20, pp. 4767-4770, 2016.
[16] D. Y. Tang, L. M. Zhao, B. Zhao, and A. Q. Liu, “Mechanism of multisoliton formation and soliton energy quantization in passively mode-locked fiber lasers,” Phys. Rev. A, vol. 72, no. 4, pp. 043816, 2005.
[17] W. J. Tomlinson, R. H. Stolen, and A. M. Johnson, “Optical wave breaking of pulses in nonlinear optical fibers,” Opt. Lett., vol. 10, no. 9, pp. 457-459, Sep. 1985.
[18] X. Liu, “Hysteresis phenomena and multipulse formation of a dissipative system in a passively mode-locked fiber laser,” Phys. Rev. A, vol. 81, no. 2, p. 023811, Feb. 2010.
[19] Y. Peiguang, L. Rongyong, Z. Han, W. Zhiteng, C. Han, and R. Shuangchen, “Multi-pulses dynamic patterns in a topological insulator mode-locked ytterbium-doped fiber laser,” Opt. Commun., vol. 335, pp. 65–72, Jan. 2015.
[20] A. M. Perego, “High-repetition-rate, multi-pulse all-normal-dispersion fiber laser,” Opt. Lett., vol. 42, no. 18, pp. 3574-3577, Sep. 2017.
[21] N. Tarasov, A. M. Perego, D. V. Churkin, K. Staliunas, and S. K. Turitsyn, “Mode-locking via dissipative Faraday instability,” Nat. Commun., vol. 7, pp. 12441, 2016.
[22] Z. Liu, Z. M. Ziegler, L. G. Wright, and F. W. Wise, “Megawatt peak power from a Mamyshev oscillator,” Optica, vol. 4, no. 6, p. 649-654, Jun. 2017.
[23] A. Komarov, F. Amrani, A. Dmitriev, K. Komarov, and F. Sanchez, “Competition and coexistence of ultrashort pulses in passive mode-locked lasers under dissipative-soliton-resonance conditions,” Phys. Rev. A, vol. 87, no. 2, p.023838, Feb. 2013.
[24] A. Niang, G. Semaan, F. B . Braham, M. Salhi, and F. Sanchez, “Dynamics of dissipative soliton resonance square pulses in fiber lasers,” Int. Conf. Transparent Opt. Networks, vol. 28, no. 1, pp. 2–5, 2017.
[25] Y. Lyu, X. Zou, H. Shi, C. Liu, C. Wei, J. Li, H. Li, and Y. Liu, “Multipulse dynamics under dissipative soliton resonance conditions,” Opt. Express, vol. 25, no. 12, pp. 13286-13295, Jun. 2017.
[26] G. Semaan, A. Niang, M. Salhi, and F. Sanchez, “Harmonic dissipative soliton resonance square pulses in an anomalous dispersion passively mode-locked fiber ring laser,” Laser Phys. Lett., vol. 14, no. 5, p.055401, May. 2017.
[27] C. Shang, X. Li, Z. Yang, S. Zhang, M. Han, and J. Liu, “Harmonic dissipative soliton resonance in an Yb-doped fiber laser,” J. Lightwave Technol., vol.36, no.20, pp. 4932-4935, Oct. 2018.
[28] Y. Lyu, H. Shi, C. Wei, H. Li, J. Li, and Y. Liu, “Harmonic dissipative soliton resonance pulses in a fiber ring laser at different values of anomalous dispersion,” Photon. Res., vol. 5, no. 6, pp. 612-615, Dec. 2017.
[29] S. Das Chowdhury, A. Pal, S. Chatterjee, R. Sen, and M. Pal, “Multipulse Dynamics of Dissipative Soliton Resonance in an All-Normal Dispersion Mode-Locked Fiber Laser,” J. Lightwave Technol., vol. 36, no. 24, pp. 5773–5779, Dec. 2018.
[30] X. Fan, S. Wang, Y. Wang, D. Shen, D. Tang, and L. Zhao, “Pump hysteresis and bistability of dissipative solitons in all-normal-dispersion fiber lasers,” vol. 54, no. 12, pp. 3774–3779, 2015.
[31] X. Liu, L. Wang, X. Li, H. Sun, A. Lin, K. Lu, Y. Wang, and W. Zhao, “Multistability evolution and hysteresis phenomena of dissipative solitons in a passively mode-locked fiber laser with large normal cavity dispersion.,” Opt. Express, vol. 17, no. 10, pp. 8506–8512, May. 2009.
[32] Y. Xu, Y. -L. Song, G. -G. Du, P. -G. Yan, C. -Y. Guo, G. -L. Zheng, and S. -C. Ruan, “Dissipative soliton resonance in a wavelength-tunable thulium-doped fiber laser with net-normal dispersion,” IEEE Photonics J., vol. 7, no. 3, p.1502007, 2015.
[33] H. Lin, C. Guo, S. Ruan, and J. Yang, “Dissipative soliton resonance in an all-normal-dispersion Yb-doped figure-eight fibre laser with tunable output,” Laser Phys. Lett., vol. 11, no. 8, pp. 085102, Aug. 2014.
[34] W. Lin, S. Wang, S. Xu, Z.-C. Luo, and Z. Yang, “Analytical identification of soliton dynamics in normal-dispersion passively mode-locked fiber lasers: from dissipative soliton to dissipative soliton resonance,” Opt. Express, vol. 23, no. 11, pp. 14860-14875, Jun. 2015.
[35] Z. Cheng, H. Li, and P. Wang, “Simulation of generation of dissipative soliton, dissipative soliton resonance and noise-like pulse in Yb-doped mode-locked fiber lasers,” Opt. Express, vol. 23, no. 5, pp. 5972-5981, Mar. 2015.
[36] Y.-Q. Huang, Y.-L. Qi, Z.-C. Luo, A.-P. Luo, and W.-C. Xu, “Versatile patterns of multiple rectangular noise-like pulses in a fiber laser,” Opt. Express, vol. 24, no. 7, pp. 7356-7363, 2016.
[37] C. Aguergaray, A. Runge, M. Erkintalo, and N. G. R. Broderick, “Raman-driven destabilization of mode-locked long cavity fiber lasers: fundamental limitations to energy scalability,” Opt. Lett., vol. 38, no. 15, pp. 2644-2646, Aug. 2013.
[38] J. -H. Cai, S. -P. Chen, and J. Hou, “1.1-kW Peak-Power Dissipative Soliton Resonance in a Mode-Locked Yb-Fiber Laser,” IEEE Photon. Technol. Lett., vol. 29, no. 24, pp. 2191–2194, Dec. 2017.
[39] H. Yu, X. Wang, P. Zhou, X. Xu, and J. Chen, “Raman continuum generation at 1.0–1.3 μm in passively mode-locked fiber laser based on nonlinear polarization rotation,” Appl. Phys. B, vol. 117, no. 1, pp. 305–309, Oct. 2014.
[40] J. Limpert, F. Roser, S. Klingebiel, T. Schreiber, C. Wirth, T. Peschel, R. Eberhardt, and A. Tunnermann, “The Rising Power of Fiber Lasers and Amplifiers,” IEEE J. Sel. Top. Quantum Electron., vol. 13, no. 3, pp. 537–545, 2007.
[41] I. N. Duling, “All-fiber ring soliton laser mode locked with a nonlinear mirror,” Opt. Lett., vol. 16, no. 8, pp. 539-541, 1991.